Low-Noise Photoplethysmography Sensor Using Correlated Double Sampling for Heartbeat Interval Acquisition

Watanabe, Kento ; Izumi, Shintaro ; Sasai, Kana ; Yano, Yuji ; Kawaguchi, Hiroshi ; Yoshimoto, Masahiko

Low-Noise Photoplethysmography Sensor using Correlated Double Sampling for Heartbeat Interval Acquisition

Kento Watanabe, *Student Member, IEEE*, Shintaro Izumi, *Member, IEEE*,
Kana Sasai, *Student Member, IEEE,* Yuji Yano,
Hiroshi Kawaguchi, *Member, IEEE*, and Masahiko Yoshimoto, *Member, IEEE*

Abstract—This study designs a low-power photoplethysmography (PPG) sensor based on the error compensation method for heartbeat interval acquisition. To perform heartbeat monitoring in daily life, it is necessary to obtain long-term and accurate heartbeat interval data with low power consumption, because of the limited size and battery capacity of the PPG sensor. Effective reduction in the power consumption of the sensor requires the duty-cycled LEDs and lowering pulse repetition frequency (PRF), *i.e.* decreasing the sampling rate. However, these methods reduce the accuracy of the heartbeat interval measurement because of signal-to-noise ratio (SNR) degradation and sampling errors. We propose an algorithm for heartbeat interval error compensation and incorporate a low-noise readout circuit to improve SNR. The readout circuit uses current integration to achieve low duty-cycle LED driving. A correlated double sampling (CDS) is introduced to minimize the random noise arising from the switching operation of the integration circuit. An error compensation method based on the PPG waveform similarity is also introduced using the autocorrelation and linear interpolation. The measurement results obtained from nine subjects show that a total current consumption of 28.2 μA is achieved with a 20-Hz PRF and 0.3% LED duty cycle. The proposed design effectively reduces the mean absolute error (MAE) of the heartbeat interval to an average of 6.2 ms.

Index Terms—Current integration circuit, heartbeat interval, LED power reduction, low-power sensor, photoplethysmogram (PPG), sampling error compensation

I. INTRODUCTION

Progressive diseases, such as stroke, angina pectoris, and myocardial infarction, are often associated with lifestyle [1]. Thus, daily monitoring of physical and mental health is expected to raise health awareness, and lead to improved lifestyle habits [2]. Recently, many wearable sensors have been developed to achieve daily lifestyle monitoring [3].

Fluctuations in heartbeat intervals are closely related to people's daily health status. It has been reported that heart rate variability analysis (HRVA) can recognize fatigue and stress conditions; it also can be utilized to detect drowsiness and diseases arising from fatigue and stress conditions [4, 5]. To measure the heartbeat interval, the R-wave interval (RRI) obtained from an electrocardiograph (ECG) is mainly used [6, 7]. Prior studies report that the pulse to pulse interval (PPI) obtained using photoplethysmography (PPG) can also be used for HRVA [8–11].

The PPG sensor can efficiently measure heartbeat without electrodes. It radiates light to the body surface using LED and measures the amount of reflected light using a photo diode. As the incident light is absorbed by the skin tissue and the hemoglobin in the blood vessels, the change in the blood volume due to the beats of the heart can be measured from the change in intensity of reflected light [12, 13]. Green light is popularly used because it balances the absorbance and penetration of light [14]. Therefore, it can be easily implemented in wearable devices such as smartphones, smart bands, and smart rings [15, 16]. However, the size of the wearable sensors and their battery capacity are strictly limited; thus, it is necessary to reduce power consumption to prolong the battery life.

Because the LED and readout circuit are responsible for the most power consumption in the wearable device, an effective way to reduce the power consumption of the PPG sensor is to reduce both the duty cycle of the LED and the pulse repetition frequency (PRF). However, these methods reduce the accuracy of the heartbeat interval measurement, because of the signal-to-noise ratio (SNR) degradation and sampling error.

To overcome the challenge arising from the ultra-low LED duty cycle, we proposed a PPG measurement system, which combined a circuit for low power operation and an algorithm for accurately extracting the heartbeat interval to improve the SNR. PPG sensors generally use a transimpedance amplifier (TIA) or a readout circuit in which an integration circuit is connected to the subsequent stage of the TIA. Previously
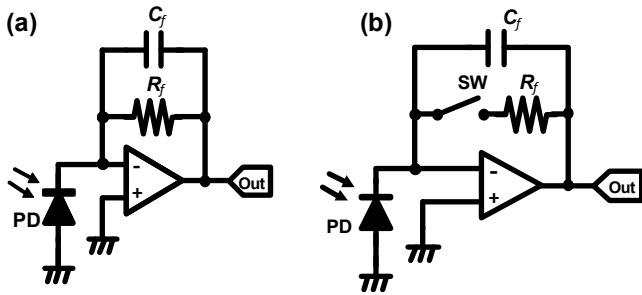
Fig. 1. Photo detection circuit (a) using transimpedance amplifier(TIA) and (b) using current integration circuit.

published work [17], analyzed shot noise, thermal noise, flicker noise, and quantization noise generated in the PPG readout chain, and reported that the current integration circuit (see Fig. 1 (b)) has better noise characteristics in comparison with TIA (see Fig.1 (a)). Therefore, we propose a PPG measurement method that can operate at an extremely low active rate by combining correlated double sampling (CDS) and autocorrelation techniques along with the use of a current integration circuit as the first stage. In addition, we included a sampling error compensation method using autocorrelation and linear interpolation to reduce the heartbeat interval error caused by the sampling error [18]. The system level performance was evaluated on nine subjects.

A preliminary version of this study has been reported in the literature [19]. This paper presents additional details on the proposed methods, an improved version of the prototype, and the performance evaluation results using measurement data of nine subjects. Section II describes the overview of the conventional PPG sensor for the wearable heartbeat monitoring device. The properties of the proposed low-noise PPG sensor design are detailed in Section III. The performance evaluation results using the prototype sensor are described in Section IV, and the results are discussed in Section V. Finally, the conclusions are presented in Section VI.

II. RELEVANT WORKS

A. Noise Reduction Methods

Noise reduction is a key component of wearable sensors. Prior studies reduced noises, such as the fluctuation of the direct current (DC) component due to the change in the contact pressure of the PPG sensor and ambient light [20-24], the motion artifact (MA) [25], and noise arising owing to sensor components [26].

A technique that combines CDS and an integration circuit connected after the TIA, has been proposed to eliminate the noise arising from ambient light [23]. A method for reducing noise caused by a circuit by using a current integration circuit and a time digital converter (TDC) instead of a TIA as a current to voltage converter has also been proposed [26]. By using TDC to construct a mechanism similar to that of CDS, the jitter caused by the current integration circuit was eliminated.

In addition, for the acquisition of the heartbeat interval, lowering the sampling rate also causes a large sampling error. However, many previous studies have aimed to measure PPG waveforms with low power consumption, and rarely mention
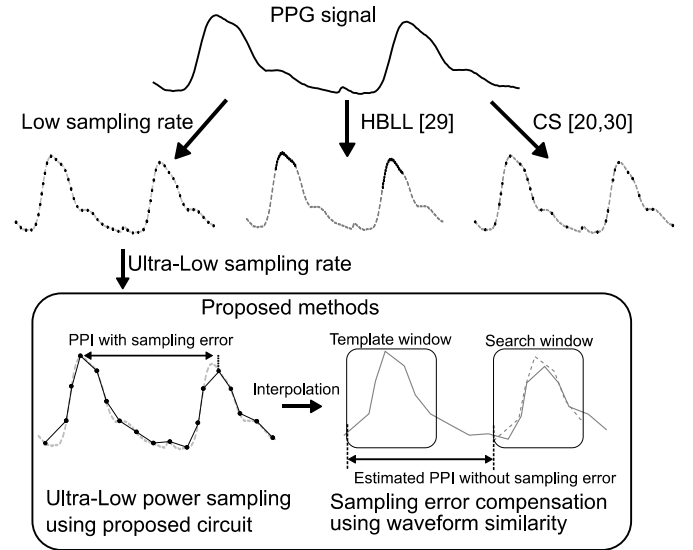

Fig. 2. Overview of reported methods of power reduction in PPG circuits. The proposed method can reduce the power consumption further by using ultra-low sampling rate and sampling error compensation.

errors caused by the sampling rate.

B. Power Reduction Methods for Heartbeat Interval Acquisition

As mentioned in Section I, it is very important to reduce the power consumption of the PPG sensor. This can be achieved by reducing the duty cycle of the LED, which consume the most power in the PPG sensor.

Fig. 2 shows three conventional LED power reduction methods. In previous studies, power consumption was generally reduced by lowering the duty cycle of the LED and PRF, and performing pulse width modulation (PWM), resulting in an LED duty cycle of about several percent. Although this considerably reduces power consumption, LED driving still consumes tens to hundreds of µW [27, 28].

In literature [29], the next peak of the PPG is estimated from the previous heartbeat interval. The LED is turned on only in the vicinity of the estimated peak and is turned off again when the peak is detected. Therefore, it is possible to reduce the power consumption without significantly reducing the sampling rate. However, the peak detection and estimation may fail, because of the noise contamination or the irregular peak interval caused by arrhythmia such as extrasystole.

Compressed sampling (CS) is used to reduce the sampling and duty cycle of the LED [20, 30]. This method can reduce the sampling rate below the Nyquist frequency by assuming a sparsity of the PPG signal in the frequency domain. The PPG signal can be transformed and reconstructed using the matrix operation [30]. The power dissipation in the reconstruction process is negligible, because it may be performed in a gateway (e.g. smartphone) or on a server. However, the heartbeat interval error becomes large by using this method, because the waveform cannot be completely reconstructed. The other method in [20] focused on the frequency component of the PPG signal and proposed a method for obtaining the heart rate directly from the compressed sampled data by extracting the

peak frequency without reconstructing the waveform. Although sampling at 4 Hz on average is possible at the minimum, only average heart rates can be obtained. It is difficult to use the average heart rate for HRV analysis.

III. PROPOSED DESIGN FOR LOW-NOISE PPG ACQUISITION

As explained above, the various approaches that have been proposed to reduce the power consumption of the PPG sensor focus mainly on reducing the duty cycle of the LED.

Here, T_{sample} and T_{LED}, respectively, denote the sampling interval and time duration of activating the LED for each sampling. Then, the duty cycle of the LED is expressed as T_{LED}/T_{sample}. Because the average energy consumption of the LED is linearly proportional to the duty cycle, the easiest way to reduce power consumption is to shorten T_{LED} and expand the T_{sample}. However, the signal-to-noise ratio (SNR) of the obtained PPG deteriorates when the duty cycle of the LED is reduced; this degrades the accuracy of the heartbeat interval obtained using the PPG.

The objective of this research is to extracting accurate heartbeat interval with a low power PPG measurement method by low LED duty cycle. The following subsections A and B present T_{LED} reduction methods and the subsection C presents a heartbeat interval error compensation method for low PRFs.

A. Current to Voltage Converter Design

First, a current integration circuit (see Fig. 1 (b)) is incorporated into the readout circuit in place of the TIA as a current to voltage converter. As described in Section I, the TIA is generally utilized in the PPG sensor. In some previous studies, the current integration circuit is connected to the next stage of the TIA to remove the instantaneous high-frequency noise, such as thermal noise [20, 23, 29, 31, 32].

Fig. 3 depicts the simulation circuit configurations and the simulation results of the output waveforms using LTspice simulator. An operational amplifier (OPA349, Texas Instruments, Dallas, TX, USA) spice model was used in the simulation, because this operational amplifier was used in our prototype, as mentioned in Section IV. As it was assumed that the LED was duty-cycled, the current from the photodiode equivalent circuit was pulsed and used as an input signal. The current value when the pulse was turned on and off was changed by several parameters. T_{LED} and T_{SW} were set to 150 μs, and C_f of the current integration circuit was set to 100 pF. The rise and fall time of the current pulse were set to 10 μs.-For comparison purposes, the gain of the current integration circuit and TIA gain were designed to be equal, and C_f of the TIA was calculated from [33].

As shown in Fig. 3 (a), TIA fluctuates for a long period due to the effect of noise in the first stage, although an optimum capacitor is selected. Therefore, it also affects integration circuits in the second stage. To sample low noise signals, it is more ideal to enable a slightly longer T_{LED}. This can cause an increase in LED power consumption. In contrast, Fig. 3 (b) show that the fluctuation duration of the first stage integration and its influence on the second stage amplifier are limited.
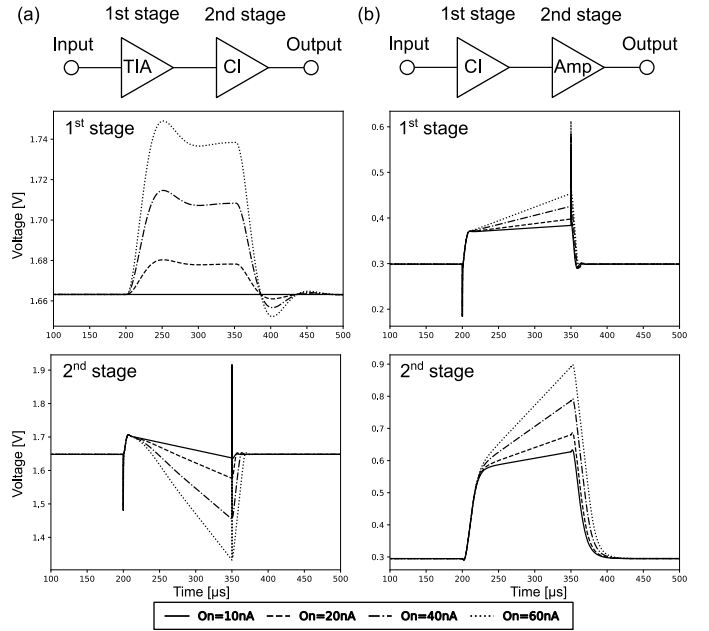

Fig. 3. Simulation results of (a) TIA with current integration (CI) and (b) CI with noninverting amplifier. A pulse current is applied assuming 150-μs T_{LED} and T_{SW} duty-cycled LED operation. Rise and fall time are set to 10 μs. On pulse current is set to 10, 20, 40 and 60 nA, and off current is set to 10 nA.

The switching noise cancellation method is discussed in Section III B. Furthermore, similar to the TIA based PPG sensor, if the ambient light is constant, its effect is superimposed on the measured value as a DC component. The ambient light also appears as noise when its levels change. The content of this paper does not deal with ambient light cancellation, but the proposed sensor can be combined with the previously proposed ambient light cancellation method for conventional PPG sensors [20].

Based on these results, the current integration circuit, which can lower the LED duty cycle, is employed in this work.

B. Switching Noise Reduction using Correlated Double Sampling

Fig. 4 (a) shows the current integration circuit output. The envelope waveform indicates the PPG signal. Fig. 4 (b) shows the waveform obtained by expanding the measurement sample of Fig. 4 (a). The output voltage is contaminated by the switching noise when the reset switch is turned from on to off. In particular, the noise is integrated when the switch is turned off, and the peak value includes the noise component. This noise component is not constant, and has sufficiently wide fluctuation compared with the PPG signal when the duty cycle of the LED is low. On the other hand, the influence of the switching noise is limited at other periods of LED driving.

To reduce the switching noise, we introduce a correlated double sampling (CDS) technique (see, Fig. 5). The CDS technique was originally proposed for charge-coupled devices to eliminate the thermal noise [34]. In this method, the noise component affecting the output as an offset is initially sampled; a second sampling is conducted after charge accumulation. The difference between these two sampling results is used as a signal [35]. In literature [34], this operation is performed using the sample and hold circuit. The switching noise in the proposed
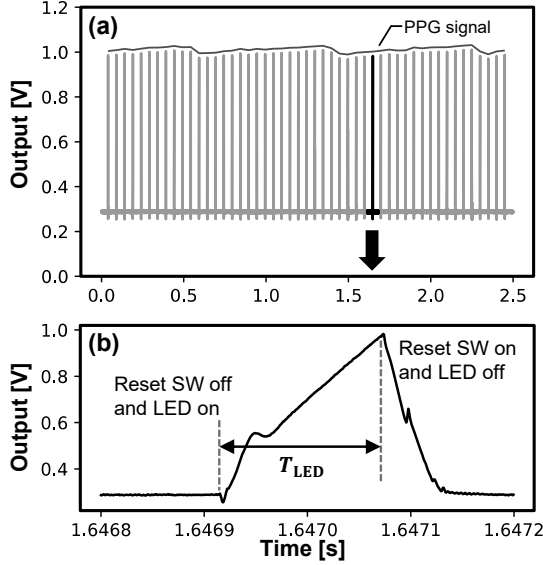
Fig. 4. (a) Example of current integration circuit output including switching noise and (b) enlarged waveform of one sampling period. Reset switch and LED are controlled periodically.
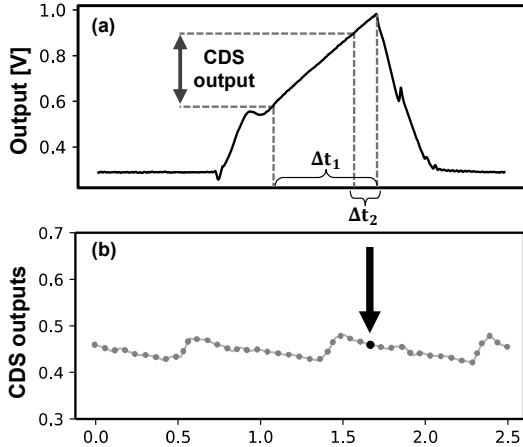

Fig. 5. (a) Applying CDS to the output of the integration circuit. The difference in sampled voltages is used as the CDS output. (b) Time series of the CDS output values compose the PPG signal excluding the switching noise.

PPG sensor (see Fig. 4 (b)) can be suppressed in the same manner. The proposed circuit samples the integration circuit output twice at short intervals (Δt_1 and Δt_2) by an analog to digital (A/D) converter, and the difference between these voltages is used as shown in Fig. 5. In other words, it uses the slope of the integral waveform (see Fig. 5 (a)), instead of its peak voltage, to obtain the PPG signal.

C. Sampling Error Compensation using Autocorrelation

Although the switching noise can be suppressed by the CDS, the sampling error still remains in the CDS output. Sampling error compensation is necessary because large sampling error is caused by increasing the sampling interval T_{sample} for power reduction.

Generally, when extracting the heartbeat interval from the PPG, the peak of the waveform is detected as shown in Fig. 2, and its interval is calculated. The sampling error that correlates
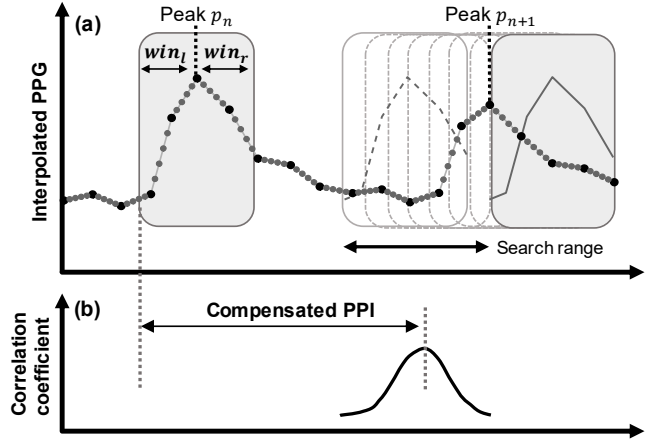

Fig. 6. Error compensation technique using autocorrelation: (a) example of CDS outputs with window definitions, (b) sampling error compensation using correlation coefficient.

with T_{sample} is superimposed on this peak interval. To mitigate this problem, it is effective to adopt autocorrelation using not only the peaks but also the entire heartbeat waveforms in the PPG. In our prior study [18], a sampling error compensation algorithm for ECG using interpolation and autocorrelation has been proposed. In this study, we apply this algorithm to the PPG.

Fig. 6 depicts the sampling error compensation algorithm. First, the PPG waveform with low sampling rates is up-converted using linear interpolation. Next, the correlation between the two windows which is generated based on p_n and p_{n+1}, within the search range centered on the detected peak is calculated as follows (1):

$$\text{Cor}(s) = \sum_{i=-win_l}^{win_r} x(p_n + i)x(p_{n+1} + s + i) \qquad (1)$$

Here, x is the zero-means-normalized input signal; p_n is the peak corresponding to the nth period; win_l and win_r are the window size for autocorrelation; and s is the window shift amount. The correlation coefficient at its maximum is used as the corrected peak. Then, using p_{n+1} as a reference of the next template window, a search window is generated from p_{n+2} and the next heartbeat interval is compensated. In this study, the search range is set to $\pm T_{\text{sample}}$, and the sampling rate of interpolation is set to 1000 Hz; thus, the values of win_l and win_r are same as the number of calculating points by autocorrelation. Because the PPG waveforms are similar to some extent, the sampling error can be compensated using this method.

IV. PERFORMANCE EVALUATION

A. Evaluation Method

To evaluate the accuracy and power consumption of our proposed system, we create a prototype of the proposed PPG sensor. Fig. 7 shows the circuit block diagram of the prototype consisting of a PIN photodiode (VEMD5510CF, Vishay Intertechnology, Malvern, PA, USA), a green LED (AM2520ZGC09, Kingbright, New Taipei City, Taiwan), a switch (TS5A3167, Texas Instruments, Dallas, TX, USA),
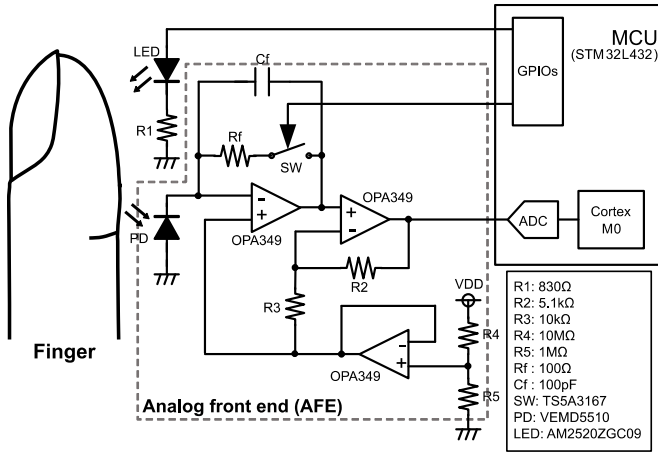
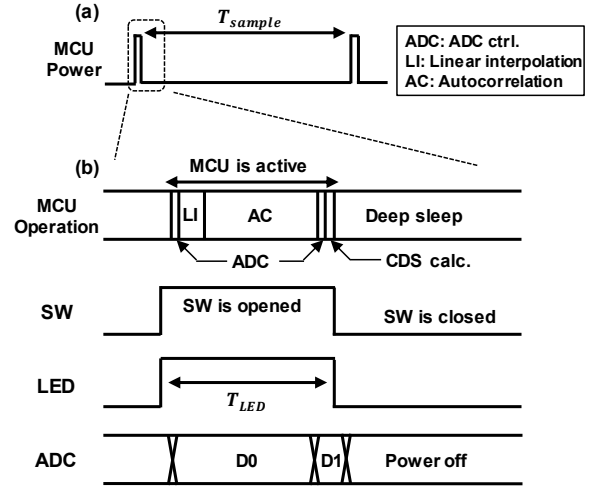Fig. 7. Circuit block diagram of prototype sensor board.

Fig. 8. Timing chart of activities of the different components in the sensor system.
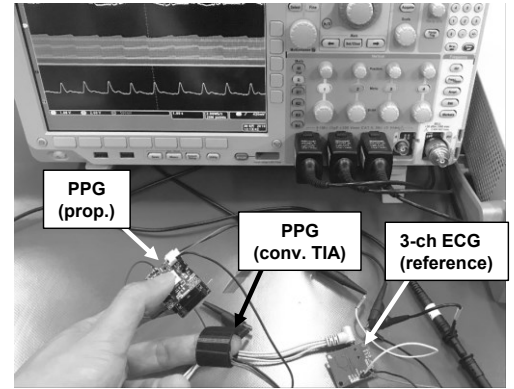

Fig. 9. Experimental setup for performance evaluation

TABLE I
PARAMETER VALUE CANDIDATES EVALUATED IN PRELIMINARY EXPERIMENT

T_{LED}	Δt_1	Δt_2	win_l	win_r
50 µs to 200 µs (50-µs step)	$0.6 \times T_{LED}$ to $0.9 \times T_{LED}$ ($0.1 \times T_{LED}$ step)	2 µs, 5 µs, 10 µs, 15 µs	100 ms to 400 ms (20 ms step)	-100 ms, to 300 ms (20 ms step)

operational amplifiers (OPA349, Texas Instruments, Dallas, TX, USA) for a current integration circuit, a non-inverted amplification circuit and a bias voltage generation circuit, and a micro controller unit (MCU) with a built-in A/D converter (STM32L432, STMicroelectronics, Geneva, Switzerland). The operating voltage of the circuit of both the analog circuit and MCU is 3.3 V, and is generated from a 3.7-V lithium-ion battery and low-dropout regulator (LDO) (TPS78330, Texas Instruments, Dallas, TX, USA). Fig. 8 illustrates the timing chart of the proposed PPG sensor. The MCU is in a deep sleep mode most of the time, and wakes up with a real-time counter (RTC) at the time of sampling. The MCU uses GPIO to control LEDs and switches, performs A/D conversion, and calculates the difference between the two sampled values, linear interpolation, and autocorrelation. The values sampled before are interpolated and autocorrelation is performed when the MCU is active. The LED is duty cycled at a constant current value (approximately 1 mA). Fig. 9 shows the experimental environment. A 3-ch ECG sensor with Ag/AgCl electrodes is used as a reference for this experiment. A commercially available PPG sensor incorporating conventional TIA [36] is also measured simultaneously using an oscilloscope (MDO4104, Tektronix, Beaverton, OR, USA) and the accuracy of the proposed system is evaluated in comparison with it.

The mean absolute error (MAE) of each heartbeat interval measured using the proposed design and the conventional PPG sensor is evaluated against the reference ECG sensor. The MAE is expressed using the following equation:

$$MAE = \frac{1}{n} \sum_{i=1}^{n} |PPI_i - RRI_i| \qquad (2)$$

Here, RRI_i is the i-th heartbeat interval according to the ECG, and PPI_i is the i-th heartbeat interval according to the PPG. n is the number of data.

To determine the appropriate parameters of the proposed circuits and algorithms (e.g. window length), preliminary experiments were conducted with three healthy subjects (2 males: 23 and 34 years old, and 1 female: 23 years old). After the parameters were determined, the MAE and power consumption are evaluated with nine subjects (five males and

four females, age: 22 to 38). In each experiment, measurement was conducted on the subjects five times for 100 s under each condition.

B. Parameters Determination

As described in Section III, the proposed PPG has the following parameters: LED lighting time, T_{LED} (see Fig. 4), CDS timing, Δt_1 and Δt_2 (see Fig. 5), and window sizes of the error correction algorithm, win_l and win_r (see Fig. 6 and (1)). These parameters are determined in this subsection according to the preliminary experiments with the three subjects.

Table I shows the candidate values of each parameters evaluated in the experiment. The three candidate values of T_{LED}, Δt_1, and Δt_2 are changed independently. The range of the window size (win_l and win_r) is set to include the rising edge of the heartbeat waveform.

TABLE II
SELECTED CDS PARAMETERS TO MINIMIZING MAE IN EACH T_{LED} WITH 250-HZ SAMPLING RATE.

T_{LED}	Δt_1	Δt_2	MAE w/ CDS	MAE w/o CDS
200 µs	160 µs	2 µs	7.10 ms	7.58 ms
150 µs	135 µs	2 µs	7.82 ms	8.04 ms
100 µs	90 µs	2 µs	12.12 ms	14.22 ms
50 µs	30 µs	2 µs	38.86 ms	38.47 ms

TABLE III
SELECTED WINDOW PARAMETERS TO MINIMIZING MAE IN EACH T_{LED} WITH 20-HZ SAMPLING RATE

T_{LED}	Δt_1	Δt_2	win_l	win_r	MAE
200 µs	160 µs	2 µs	300 ms	60 ms	5.45 ms
150 µs	135 µs	2 µs	320 ms	40 ms	5.55 ms
100 µs	90 µs	2 µs	360 ms	260 ms	7.49 ms

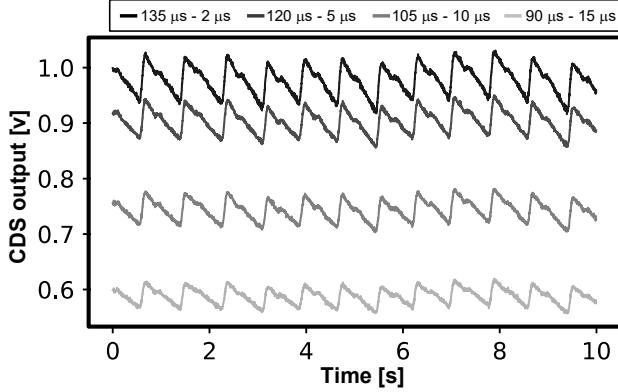Fig. 10. Raw PPG waveform with each CDS parameters. Then, T_{LED} and sampling rate are respectively set to 150 µs and 250 Hz.
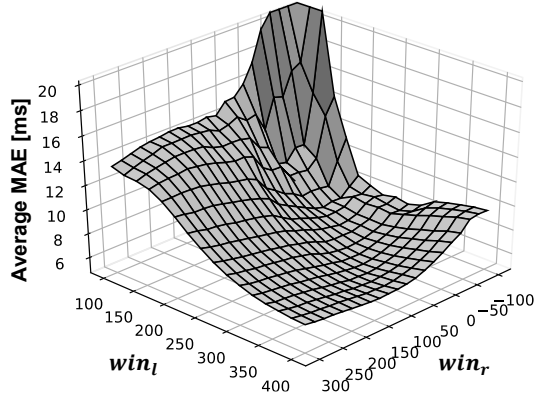

Fig. 11. Relationship between MAE and window parameters at 150-µs T_{LED}
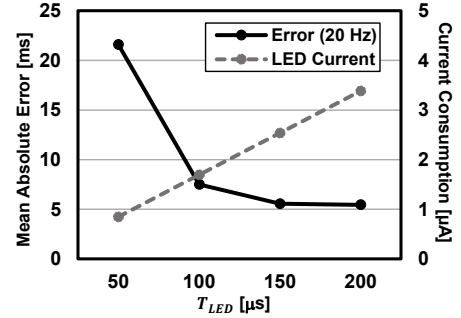

Fig. 12. Influence of LED driving duration T_{LED}

CDS parameters shown in Table II are used in the evaluation. The sampling rate is set to 20 Hz to evaluate the error compensation performance at low sampling rates. Fig. 11 shows the MAE for each window width when the T_{LED} is set to 150 µs. This result shows that the error decreases as win_l increases, and win_r has the smallest error in the region near zero.

The optimal window width for each T_{LED} is shown in Table III. The result shows that the minimum error can be achieved with approximately 300-ms win_l and 50-ms win_r at 150-µs T_{LED}. This result indicates that it is necessary to include the rising edge, and the maximum and minimum values of the heartbeat waveform in the window. In the case of a bimodal peak, it is more accurate to exclude the latter peak.

The relationship between the MAE and the power consumption of the LED in each T_{LED} is shown in Fig. 12. This result indicates that at least 150-µs T_{LED} is required to maintain the minimum MAE. Then, the duty cycle of the LED is 0.3% at 20-Hz sampling rate, and the LED current consumption is 2.5 µA.

C. Performance Evaluation

According to the preliminary experiment results shown in Section IV (b), we determined the CDS parameters as T_{LED} = 150 µs, Δt_1 = 135 µs, and Δt_2 = 2 µs. The window parameters win_l and win_r are also respectively set to 320 ms and 40 ms. Next, we conducted the performance evaluation with nine subjects to obtain more accurate MAE and reduce the total power consumption of the proposed PPG sensor.

The relationship between the sampling interval T_{sample} and the MAE of the heartbeat interval is shown in Fig. 13. Note that the PPI has at least a MAE spanning a few milliseconds, because the pulse wave velocity is continuously changing due to variables such as body motion, body position change, and blood pressure fluctuation. The MAE of the proposed sensor is

1) Determining CDS parameters

In determining the CDS parameters, the heartbeat intervals are extracted from data measured at a sampling rate of 250 Hz, the maximum sampling rate used in this study. Then, error compensation is not performed.

Fig. 10 shows the raw PPG waveforms with some CDS parameters. As shown in Fig. 10, longer CDS intervals improves the PPG signal gain and its SNR.

Table II shows the selected CDS parameters that can minimize the MAE. Regardless of the T_{LED}, the result shows that wider CDS intervals are preferable. Several peak miss detections degrade the time error with 50-µs T_{LED} due to the waveform deterioration caused by SNR degradation. Thus, 50-µs T_{LED} was not used in the subsequent evaluation.

2) Determining Window Parameters

Next, we determine the optimal value of the window parameters for the sampling error compensation algorithm. The
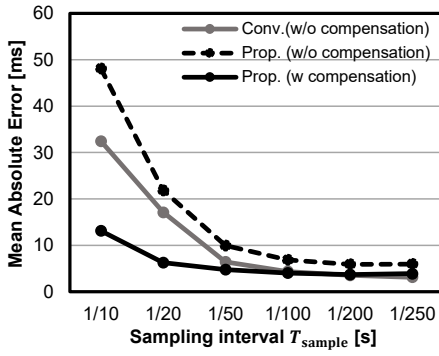
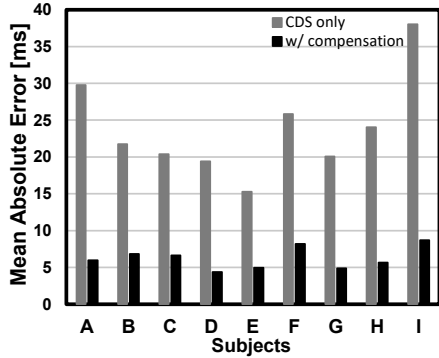Fig. 13. Relationship between sampling interval and MAE

Fig. 14. Accuracy evaluation of measurement for each subject. T_{sample} is set to 1/20s.

obtained within 7 ms, when the T_{sample} is less than or equal to 1/20 s (20-Hz sampling rate). When the T_{sample} is 1/10 s or less, accurate detection of the peak is sometimes impossible, leading to unacceptable interval error. The proposed PPG sensor without sampling error compensation achieves similar MAE, compared to the conventional PPG incorporating the TIA, despite the significant reduction of the duty cycle and power consumption of the LED. Furthermore, the sampling error compensation algorithm can be used to further reduce the MAE. Consequently, the MAE is improved by 71% when the T_{sample} is set to 1/20 s. Fig. 14 shows the MAE improvement for each subject. In practice, it is desirable to use an A/D converter clock with as high a frequency as possible to perform accurate CDS. For example, when the sampling timings fluctuated randomly in 1 μs, the MAE became 5.2 ms from 4.3 ms. However, since the timing from switching is important, it does not fluctuate so far.

Finally, the power consumption of the proposed PPG sensor is evaluated. The current consumption is measured by source measure unit (B2912A, Agilent Technologies, Santa Clara, CA, USA). Fig. 15 shows the measured current consumption of the prototype sensor board, and it achieves 28.2-μA total current consumption except for data transmission. Although the LED consumes the most power in the conventional PPG sensor, it consumes only 2.5 μA in the proposed PPG sensor due to the duty cycle of 0.3%. The current-consumption of the analog circuit and MCU were 3.8 μA and 21.9 μA, respectively. The clock speed of the A/D converter is 80 MHz, which is sufficiently high to perform CDS in MCU.
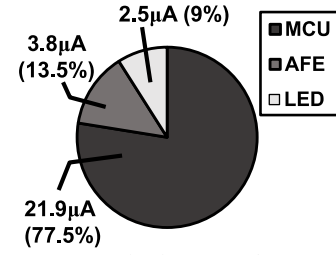

Fig. 15. Total current consumption in proposed PPG sensor

V. DISCUSSION

As shown in Section IV, the proposed PPG sensor achieves 28.2-μA total current-consumption and 6.2-ms-MAE. Table IV shows the performance comparison between the low-power PPG sensor design in this study and prior studies [20, 31, 28, 29, 32]. Prior studies used TIA as a current to voltage converter, and a switched integrator or a switched-capacitor LPF was connected to the TIA. Table IV presents the circuit that was used for the current to voltage converter. The proposed PPG sensor achieves minimal LED driving current. Although [29] exhibits less total power consumption with the minimum LED driving current, the heartbeat interval error in the study is large, as shown in Table IV. Furthermore, this method employs an adoptive active rate control, and the average power consumption is dependent on the average beat per minute (BPM), despite the fact that the power consumption of the proposed method is independent of the heartbeat interval.

The prototype sensor board does not include the communication module, and the data were extracted via a serial interface in our experiment. For wearable sensors, it is desirable to use wireless communication to transmit data. It is estimated that the required power consumption for data communication is 26 μW for raw data (20-Hz sampling) transmission, and 9 μW for extracted heartbeat interval (60 BPM) transmission, when using Bluetooth Low Energy (estimated by [37]). This power overhead is not included in the power consumptions of prior works compared in Table IV. Although the power reduction of data handling is part of our future work, the sampling reduction of the proposed method also has an advantage in this regard because the transmitting data size directly affects the transmission energy consumption.

The operational amplifiers used in the proposed sensor have limited performance (e.g. input referred noise) because we assign a higher priority to its power consumption. However, the PPG performance is not determined only by that performance but by the entire system which includes PD, LED, readout circuit and signal processing. Therefore, we prototype the proposed PPG measurement system for heartbeat interval acquisition and the real-time measurement evaluation was conducted on nine subjects. Compared to previous studies, this study achieves sufficient accuracy and low current consumption. (see Table IV).

Many previous studies use BPM as an error indicator. However, it is difficult to directly compare the MAE, because the time error of the heartbeat interval depends on the instantaneous heart rate. For example, 5-BPM correlates to

TABLE IV
PERFORMANCE COMPARISON TABLE

|	[20]	[31]	[28]	[29]	[32]	**This work**
Current to voltage conversion-method	TIA	TIA	TIA	TIA	TIA	**Current Integration**
Pulse repetitive frequency	128, 16, 13 and 4 Hz	N/A	128 Hz	40, 100 Hz	100 Hz	**20 Hz**
Supply voltage	1.2 V	1.5 V and 3.3 V (LED) 1.2 V (Digital)	0.5 V	3.3 V	3.3 V	**3.3 V**
LED operation method (LED duty cycle)	CS based (N/A)	duty-cycled (1%)	pulse density modulation (N/A)	peak based (0.01 – 1%)	duty-cycled (3%)	**duty-cycled (0.3%)**
LED current consumption	35.8 µA	120 µA	2200 µA	2.7 – 157.6 µA	93.6 – 412 µA	**2.5 µA**
Total current consumption	179.2 µA	155.8 µA	2206 µA	11.5 – 165.9 µA	253.6 – 572.1 µA	**28.2 µA**
Total power consumption	215 µW	446 µW	1100 µW	38.1 – 509.1 µW	837 – 1888 µW	**93.1 µW**
Feature extraction	Heart rate	Heart rate	Heart rate / HRV	Heart rate	SpO$_2$	**Heart rate**
Heartbeat interval error	2 BPM (measured)	N/A	68-ms SDNN 67-ms RMSSD	5 BPM at 40-Hz (sinusoidal wave)	N/A	**0.52 BPM and 6.2-ms MAE (measured with 9 subjects)**
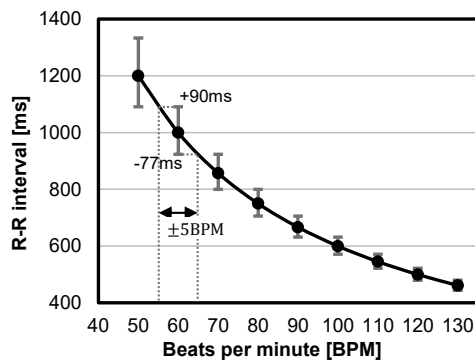
Fig. 16. Relationship between BPM and RRI error of 5 BPM

approximately 47-ms MAE when the average heart rate is 80 BPM. However, this MAE is increased to 84 ms when the average heart rate is 60 BPM, as shown in Fig. 16. Therefore, when using the BPM as an evaluation index, it is necessary to consider the average heart rate while measurement. In our study, the average heart rate is 68.9 BPM, and the error is 0.52 BPM, which is calculated according to each PPI and RRI. This error is minimal, compared with the prior studies shown in Table IV.

Fig. 17 shows the Bland–Altman plot of the heartbeats measurements of all nine subjects using the proposed PPG sensor at the sampling rate of 20 Hz. The gray dashed lines indicate the mean of the difference and agreement limits. The heartbeat interval error does not appear to have systematic errors, and the sampling error is successfully suppressed by the error compensation as shown in Fig. 17 (b).

The drawback of the proposed sensor is the current consumption of the MCU that is used for the LED and switch control, and the CDS operation. Although the prior studies integrate their readout circuits, our prototype board is composed of discrete integrated circuits (ICs). Therefore, further power reduction can be achieved by implementing such MCU functions in a dedicated hardware.

We showed the reduction of the heartbeat interval error by the proposed algorithm in actual measurements at rest.
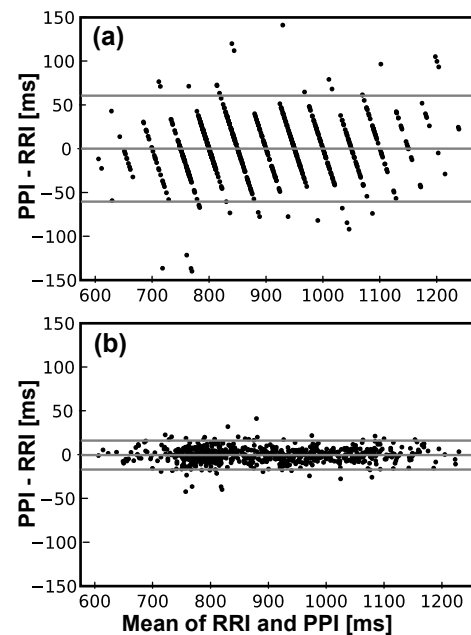

Fig. 17. Bland-Altman plot of extracted heartbeat (a) without sampling error compensation, and (b) with sampling error compensation at 20-Hz.

However, to prevent motion artifacts, the proposed method is required to be combined with other noise reduction methods. For example, the previous study [25] proposed a motion artifacts reduction method at a low sampling rate using two PPG sensors with different distances from the human skin.

Moreover, in this study, we determined common parameter values, such as window length, for all the measurement data of all the subjects. These parameters are also static, with respect to heart rate variability. However, this may diminish the accuracy when the heat rate is higher during exercise, because our experiment results show that the windows should contain the rising edge and maximum and minimum values of the heartbeat waveform to minimize the error. This challenge will be circumvented if the parameters can vary dynamically according to the heart rate.
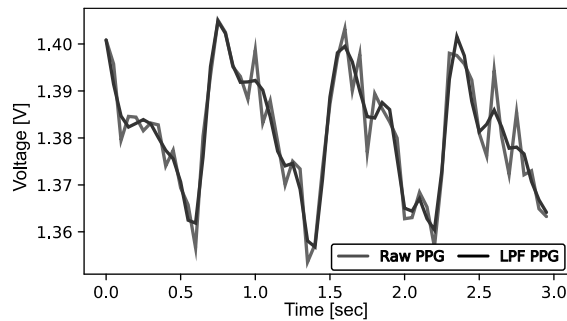
Fig. 18. Measured PPG on the wrist. The gain of second stage is changed to 10x and other parameters are fixed.

In this study, the performance was evaluated by undertaking measurements with the fingertip. The result of the measurement on the wrist is depicted in Fig. 18. MAE was 13 ms, and the error was large compared to the measurement with the fingertip. This is because the similarity of the waveform was lowered due to noise. Improving the wrist measurement accuracy is indispensable for wearable healthcare and is a future issue to be tackled.

VI. CONCLUSION

In this study, we proposed a sensing method for realizing low-power PPG for long-term heartbeat monitoring in daily life. We introduced a design that integrates the current integration circuit, CDS, and sampling error compensation based on autocorrelation and linear interpolation. Using the prototype sensor board, the accuracy and power consumption of the proposed PPG sensor were evaluated with the measurement results of nine subjects. The proposed sensor achieves 28.2-µA total current consumption and 6.2-ms MAE with 150-µs T_{LED} and 20-Hz sampling rate.

REFERENCES

[1] World Health Statistics 2018: Monitoring Health for the SDGs, World Health Org., 2018

[2] Han, Yongkoo et al. "A framework for supervising lifestyle diseases using long-term activity monitoring." *Sensors (Basel, Switzerland)*, vol. 12,5, 5363-79, Apr. 2012

[3] A. Pantelopoulos and N. G. Bourbakis, "A Survey on Wearable Sensor-Based Systems for Health Monitoring and Prognosis," in *IEEE Transactions on Systems, Man, and Cybernetics, Part C (Applications and Reviews)*, vol. 40, no. 1, pp. 1-12, Jan. 2010.

[4] K. Fujiwara *et al.*, "Heart Rate Variability-Based Driver Drowsiness Detection and Its Validation With EEG," in *IEEE Transactions on Biomedical Engineering*, vol. 66, no. 6, pp. 1769-1778, June 2019.

[5] Kim, Hye-Geum et al. "Stress and Heart Rate Variability: A Meta-Analysis and Review of the Literature." *Psychiatry investigation*, vol. 15,3, 235-245, Mar. 2018

[6] R. W. DeBoer, J. M. Karemaker and J. Strackee, "Comparing Spectra of a Series of Point Events Particularly for Heart Rate Variability Data," in *IEEE Transactions on Biomedical Engineering*, vol. BME-31, no. 4, pp. 384-387, Apr. 1984.

[7] C. Chou, S. Tseng, E. Chua, Y. Lee, W. Fang and H. Huang, "Advanced ECG processor with HRV analysis for real-time portable health monitoring," *2011 IEEE International Conference on Consumer Electronics -Berlin (ICCE-Berlin)*, Berlin, 2011, pp. 172-175.

[8] L. Iozzia, L. Cerina, and L. Mainardi, "Relationships between heart-rate variability and pulse-rate variability obtained from video-PPG signal using ZCA," *Physiological Measurement*, vol. 37, no. 11, pp. 1934–1944, Sep. 2016.

[9] S. Lu, H. Zhao, K. Ju, K. Shin, M. Lee, K. Shelley, and K. H. Chon, "Can Photoplethysmography Variability Serve as an Alternative Approach to Obtain Heart Rate Variability Information?," *Journal of Clinical Monitoring and Computing*, vol. 22, no. 1, pp. 23–29, Nov. 2007.

[10] Morelli, Davide et al. "Profiling the propagation of error from PPG to HRV features in a wearable physiological-monitoring device." *Healthcare technology letters* vol. 5,2 59-64. 12 Feb. 2018.

[11] G. Lu, F. Yang, J. A. Taylor, and J. F. Stein, "A comparison of photoplethysmography and ECG recording to analyse heart rate variability in healthy subjects," *Journal of Medical Engineering & Technology*, vol. 33, no. 8, pp. 634–641, Dec. 2009.

[12] A. Kamal, J. Harness, G. Irving, and A. Mearns, "Skin photoplethysmography — a review, "*Computer Methods and Programs in Biomedicine*, vol. 28, no. 4, pp. 257–269, Apr. 1989.

[13] Tamura, T.; Maeda, Y.; Sekine, M.; Yoshida, M., "Wearable Photoplethysmographic Sensors—Past and Present," *Electronics*, vol. *3*, no. 2, pp. 282-302, Apr. 2014.

[14] B. A. Fallow, T. Tarumi, and H. Tanaka, "Influence of skin type and wavelength on light wave reflectance," *Journal of Clinical Monitoring and Computing*, vol. 27, no. 3, pp. 313–317, Jun. 2013.

[15] J. P. Dieffenderfer *et al.*, "Solar powered wrist worn acquisition system for continuous photoplethysmogram monitoring," *2014 36th Annual International Conference of the IEEE Engineering in Medicine and Biology Society*, Chicago, IL, 2014, pp. 3142-3145.

[16] Matsumura K, Rolfe P, Lee J, Yamakoshi T, "iPhone 4s Photoplethysmography: Which Light Color Yields the Most Accurate Heart Rate and Normalized Pulse Volume Using the iPhysioMeter Application in the Presence of Motion Artifact?" PLOS ONE, vol. 9, no. 3, Mar. 2014.

[17] A. Caizzone, A. Boukhayma and C. Enz, "Comprehensive noise analysis in PPG read-out chains," *2017 International Conference on Noise and Fluctuations (ICNF)*, Vilnius, 2017, pp. 1-4.

[18] Y. Nishikawa, S. Izumi, Y. Yano, H. Kawaguchi and M. Yoshimoto, "Sampling Rate Reduction for Wearable Heart Rate Variability Monitoring," *2018 IEEE International Symposium on Circuits and Systems (ISCAS)*, Florence, 2018, pp. 1-5.

[19] K. Watanabe, S. Izumi, Y. Yano, H. Kawaguchi and M. Yoshimoto, "A 5-ms Error, 22- μ A Photoplethysmography Sensor using Current Integration Circuit and Correlated Double Sampling," *2018 40th Annual International Conference of the IEEE Engineering in Medicine and Biology Society (EMBC)*, Honolulu, HI, 2018, pp. 5566-5569.

[20] V. R. Pamula *et al.*, "A 172 µW Compressively Sampled Photoplethysmographic (PPG) Readout ASIC With Heart Rate Estimation Directly From Compressively Sampled Data," in *IEEE Transactions on Biomedical Circuits and Systems*, vol. 11, no. 3, pp. 487-496, June 2017.

[21] A. K. Y. Wong, K. Pun, Y. Zhang and K. N. Leung, "A Low-Power CMOS Front-End for Photoplethysmographic Signal Acquisition With Robust DC Photocurrent Rejection," in *IEEE Transactions on Biomedical Circuits and Systems*, vol. 2, no. 4, pp. 280-288, Dec. 2008.

[22] J. Kim, T. Lee, J. Kim and H. Ko, "Ambient light cancellation in photoplethysmogram application using alternating sampling and charge redistribution technique," *2015 37th Annual International Conference of the IEEE Engineering in Medicine and Biology Society (EMBC)*, Milan, 2015, pp. 6441-6444.

[23] M. Konijnenburg *et al.*, "A Multi(bio)sensor Acquisition System With Integrated Processor, Power Management, 8 $\times$ 8 LED Drivers, and Simultaneously Synchronized ECG, BIO-Z, GSR, and Two PPG Readouts," in *IEEE Journal of Solid-State Circuits*, vol. 51, no. 11, pp. 2584-2595, Nov. 2016.

[24] P. Schönle, F. Glaser, T. Burger, G. Rovere, L. Benini and Q. Huang, "A Multi-Sensor and Parallel Processing SoC for Miniaturized Medical Instrumentation," in *IEEE Journal of Solid-State Circuits*, vol. 53, no. 7, pp. 2076-2087, July 2018.

[25] T. Shimazaki, S. Hara, H. Okuhata, H. Nakamura and T. Kawabata, "Cancellation of motion artifact induced by exercise for PPG-based heart rate sensing," *2014 36th Annual International Conference of the IEEE Engineering in Medicine and Biology Society*, Chicago, IL, 2014, pp. 3216-3219.

[26] S. V. Gubbi and B. Amrutur, "Adaptive Pulse Width Control and Sampling for Low Power Pulse Oximetry," in *IEEE Transactions on Biomedical Circuits and Systems*, vol. 9, no. 2, pp. 272-283, April 2015.

[27] Kim, Jongpal, Jihoon Kim, and Hyoungho Ko. "Low-Power Photoplethysmogram Acquisition Integrated Circuit with Robust Light Interference Compensation." Ed. Vittorio M. N. Passaro. *Sensors (Basel, Switzerland)* vol. 16, no. 1: 46, 2016.

[28] W. Saadeh, S. Z. Aslam, A. Hina and F. Asghar, "A 0.5V PPG-based Heart Rate and Variability Detection System," *2018 IEEE Biomedical Circuits and Systems Conference (BioCAS)*, Cleveland, OH, 2018, pp. 1-4.

[29] J. Lee, D. Jang, S. Park and S. Cho, "A Low-Power Photoplethysmogram-Based Heart Rate Sensor Using Heartbeat Locked Loop," in *IEEE Transactions on Biomedical Circuits and Systems*, vol. 12, no. 6, pp. 1220-1229, Dec. 2018.

[30] P. K. Baheti and H. Garudadri, "An Ultra Low Power Pulse Oximeter Sensor Based on Compressed Sensing," *2009 Sixth International Workshop on Wearable and Implantable Body Sensor Networks*, Berkeley, CA, 2009, pp. 144-148.

[31] A. Sharma et al., "A Sub-60- µA Multimodal Smart Biosensing SoC With >80-dB SNR, 35- µA Photoplethysmography Signal Chain," in *IEEE Journal of Solid-State Circuits*, vol. 52, no. 4, pp. 1021–1033, Apr. 2017.

[32] K. N. Glaros and E. M. Drakakis, "A Sub-mW Fully-Integrated Pulse Oximeter Front-End," in *IEEE Transactions on Biomedical Circuits and Systems*, vol. 7, no. 3, pp. 363-375, June 2013.

[33] TEXAS INSTRUMENTS, "AN-1803 Design Considerations for a Transimpedance Amplifier," February 2008 "http://www.ti.com/lit/an/snoa515a/snoa515a.pdf", (accessed 27/6/2019)

[34] M. H. White, D. R. Lampe, F. C. Blaha and I. A. Mack, "Characterization of surface channel CCD image arrays at low light levels," in *IEEE Journal of Solid-State Circuits*, vol. 9, no. 1, pp. 1-12, Feb. 1974.

[35] X. Jin, "Principle of simple correlated double sampling and its reduced-area low-noise low-power circuit realization," in *Analog Integrated Circuits and Signal Processing*, vol. 65, no. 2, pp. 209–215, Nov. 2010.

[36] Pulse sensor, "https://pulsesensor.com/", (accessed 27/6/2019)

[37] Nordic Semiconductor, Inc., nRF52 online power profiler, "https://devzone.nordicsmi.com/nordic/power/"

Kento Watanabe (S'18) received B.Eng. degrees in Computer Science and Systems Engineering from Kobe University, Kobe, Japan in 2018. He is currently in the master course at Kobe University. His current research is biomedical signal processing and low power sensor design.
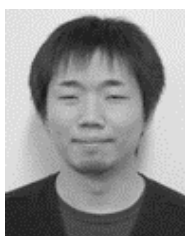
Shintaro Izumi (S'09-M'12) respectively received his B.Eng. and M.Eng. degrees in Computer Science and Systems Engineering from Kobe University, Hyogo, Japan, in 2007 and 2008. He received his Ph.D. degree in Engineering from Kobe University in 2011. He was a JSPS research fellow at Kobe University from 2009 to 2011, an Assistant Professor in the Organization of Advanced Science and Technology at Kobe University from 2011 to 2018, and an Associate Professor in the Institute of Scientific and Industrial Research at Osaka University from 2018 to 2019. Since 2019, he has been an Associate Professor in the Graduate School of System Informatics, Kobe University, Japan. His current research interests include biomedical engineering, biosignal processing, low-power circuit design, and sensor networks.

He has served as a Technical Committee Member for IEEE Biomedical and Life Science Circuits and Systems, as a Student Activity Committee Member for IEEE Kansai Section, and as a Program Committee Member for IEEE Symposium on Low-Power and High-Speed Chips (COOL Chips). He was a Chair of IEEE Kansai Section Young Professionals Affinity Group and a recipient of 2010 IEEE SSCS Japan Chapter Young Researchers Award.

Kana Sasai (S'19) received B.Eng. degrees in Computer Science and Systems Engineering from Kobe University, Kobe, Japan in 2019. She is currently in the master course at Kobe University. Her current research is low power biomedical sensor design.

Yuji Yano received the M.S. degree in electronic engineering from the Hiroshima University, Hiroshima, Japan, in 2004. In 2004 he joined the SOC Division, Renesas Technology Corp., Hyogo, Japan. Since 2016, he has been a researcher at Graduate School of System Informatics, Kobe University, Hyogo, Japan, where he has been engaged in the design and development of the ultra-low power (ULP) system LSI solutions.

Hiroshi Kawaguchi (M'98) received B.Eng. and M.Eng. degrees in electronic engineering from Chiba University, Chiba, Japan, in 1991 and 1993, respectively, and earned a Ph.D. degree in electronic engineering from The University of Tokyo, Tokyo, Japan, in 2006.

He joined Konami Corporation, Kobe, Japan, in 1993, where he developed arcade entertainment systems. He moved to The Institute of Industrial Science, The University of Tokyo, as a Technical Associate in 1996, and was appointed as a Research Associate in 2003. In 2005, he moved to Kobe University, Kobe, Japan. Since 2007, he has been an Associate Professor with The Department of Information Science at that university. He is also a Collaborative Researcher with The Institute of Industrial Science, The University of Tokyo. His current research interests include low-voltage SRAM, RF circuits, and ubiquitous sensor networks.

Dr. Kawaguchi was a recipient of the IEEE ISSCC 2004 Takuo Sugano Outstanding Paper Award and the IEEE Kansai Section 2006 Gold Award. He has served as a Design and Implementation of Signal Processing Systems (DISPS) Technical Committee Member for IEEE Signal Processing Society, as a Program Committee Member for IEEE Custom Integrated Circuits Conference (CICC) and IEEE Symposium on Low-Power and High-Speed Chips (COOL Chips), and as

an Associate Editor of IEICE Transactions on Fundamentals of Electronics, Communications and Computer Sciences and IPSJ Transactions on System LSI Design Methodology (TSLDM). He is a member of the IEEE, ACM, IEICE, and IPSJ.

Mashahiko Yoshimoto (M'02) joined the LSI Laboratory, Mitsubishi Electric Corporation, Itami, Japan, in 1977. From 1978 to1983 he had been engaged in the design of NMOS and CMOS static RAM. Since 1984 he had been involved in the research and development of multimedia ULSI systems. He earned a Ph.D. degree in Electrical Engineering from Nagoya University, Nagoya, Japan in 1998. Since 2000, he had been a professor of Dept. of Electrical & Electronic System Engineering in Kanazawa University, Japan. Since 2004, he has been a professor of Dept. of Computer and Systems Engineering in Kobe University, Japan. His current activity is focused on the research and development of an ultra low power multimedia and ubiquitous media VLSI systems and a dependable SRAM circuit. He holds on 70 registered patents.

He has served on the program committee of the IEEE International Solid State Circuit Conference from 1991 to 1993. Also he served as Guest Editor for special issues on Low-Power System LSI ,IP and Related Technologies of IEICE Transactions in 2004. He was a chair of IEEE SSCS (Solid State Circuits Society) Kansai Chapter from 2009 to 2010. He is also a chair of The IEICE Electronics Society Technical Committee on Integrated Circuits and Devices from 2011-2012. He received the R&D100 awards from the R&D magazine for the development of the DISP and the development of the realtime MPEG2 video encoder chipset in 1990 and 1996, respectively. He also received 21th TELECOM System Technology Award in 2006.